

THE HERON PROJECT

J.S. ADAMS, Y.H. HUANG, Y.H. KIM, R.E. LANOU, H.J. MARIS & G.M. SEIDEL

Department of Physics, Brown University, Providence, RI 02912, USA
E-mail: lanou@physics.brown.edu

HERON (for HELium Roton Observation of Neutrinos) is an R&D project whose aim is to have a high-rate, real-time detector of p-p and ${}^7\text{Be}$ solar neutrinos. The neutrino target material is superfluid helium—a medium which can be made free of internal radioactive background. The elastic neutrino interactions are detected by measuring, on wafer calorimeters mounted above the liquid, the UV photons and phonon/rotons generated by the recoil electron. This paper discusses the status of the project with particular emphasis on progress toward control of backgrounds from sources external to the liquid helium target volume.

1 Introduction

As the theme of this workshop implies, the discoveries in recent years in neutrino physics are pushing us to provide new techniques and new detectors to take us to the next level of understanding. This is especially true in the case of solar neutrinos where as a community we do not yet have the proven capability to measure the total flux and spectrum of the neutrinos from the p-p branch. Detailed knowledge of the p-p branch will provide a valuable component to unraveling the neutrino mass and mixing matrix as well as to our understanding of how the Sun generates its energy since the p-p reaction is the source of more than 90% of the solar neutrino flux.

To have sensitivity to the full flux of non-sterile neutrinos (ν_e , ν_μ , and ν_τ) the elastic scattering from electrons is the reaction of choice:

$$\nu_x + e^- \rightarrow \nu_x + e^- \quad (1)$$

In addition to its sensitivity to both charged and neutral currents use of reaction (1) has two other attractive features. Its cross section is very precisely known and thus the detector does not require the use of intense radioactive “calibration” sources. In contrast to inverse beta decay detection, the large total flux in combination with reaction (1) also permits very high event rates even with targets of very modest size (~ 2 events/day/tonne) relative to the current Cherenkov and liquid scintillator detectors. However, the need to detect the very low energies of the electron recoils from events due to the p-p continuum and the ${}^7\text{Be}$ -line (≤ 261 and ≤ 665 keV, respectively) presents an enormous challenge to the realization of a successful solar neutrino detector.

While extracting signals with energies this low from sizable targets is in itself a challenge the primary difficulties arise from the need to eliminate, reduce or otherwise provide a discriminating event signature from the many sources of backgrounds which increase at these low energies. Among the sources are cosmogenic and primordial isotopes in the targets or container, primordial radioactivity in the laboratory and muon induced activities in the target, shields or laboratory walls from those muons penetrating the laboratory overburden.

2 Description of HERON

The neutrino target material for HERON is superfluid helium (^4He) at ~ 50 mK. In the superfluid state, helium is self-cleaning; that is all other atomic species rapidly freeze to the walls. There are two other advantages to the low temperature: radon migration into the volume is non-existent or negligible while, because kT energy is so low, the gravitational potential of dust particles or even a single uranium atom is much greater resulting in their fall to the bottom of the container. As a consequence of all these effects the bulk material of the neutrino target can be made completely free of background originating internally.

A charged particle stopping in superfluid helium generates two useful forms of radiant energy: fast UV photons and delayed phonons/rotons. The former are strongly peaked at 16 eV, an energy below the first excited state of the helium atom and thus the liquid is transparent to the UV. At these temperatures in helium the Rayleigh scattering is negligible. The path length in the liquid for the electrons recoiling from the p-p and ^7Be neutrino elastic scatters is ≤ 2 cm thus, on the scale of the HERON detector volume (~ 64 m³) the photons are effectively from a point source. This feature is utilized in our design for purposes of event location and background discrimination. The rotons and phonons also propagate ballistically and a certain fraction of them undergo quantum evaporation (the ejection of a helium atom in a one-to-one process) at the free surface of the liquid. The multiplicity of rotons/phonons is high since their quanta have energies of order 1 meV. The kinematics of quantum evaporation confine the detectable roton/photons to a 30° half-angle cone. The UV photon and roton/phonon initiated signals are detected on arrays of thin, sapphire or silicon wafer calorimeters. In a series of experiments with 4 liter prototypes containing superfluid, we have established the physics of low energy electron and alpha particle production of UV photons and rotons and their detection on wafer calorimeters¹. Some of the results relevant to discussion of a p-p neutrino detector are contained in Table 1. In a full scale detector the wafer calorimeters (~ 12 cm diam.) would be arranged in two

Table 1. Energy division among radiation channels.

Channel	Alpha (into 4π)	Ratio (α/e)	Electron (into 4π)	Electron (E detected at wafers).
Emitted in UV (singlet; 10^{-8} s.)	10%	0.29	35%	Solid Ω dependent.
Remain in triplet (~ 10 s.)	3%	0.13	24%	—
Rotons/phonons	87%	2.12	41%	3%(Critical cone)

planes above the liquid surface. The combined UV photon and roton/phonon signals are used for the recoil energy determination while the correlations in UV photon hit patterns in the two planes are utilized to deduce the neutrino event location (single energy deposition) and to distinguish them from much of the background (multiple Compton scatters of gammas) by a method closely related to the coded apertures^{2,3} of x-ray astronomy and tomography. Our tests of the application of this method are discussed in Section 3.

Fig. 1 schematically illustrates a possible configuration of HERON and its shield. The liquid helium (5m diam. by 5 m high in this version) is

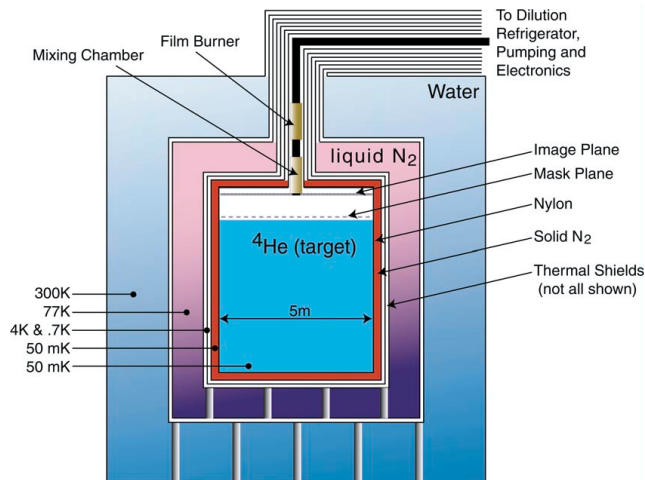


Figure 1. A possible installation of HERON within shielding (not to scale).

contained in an inner copper cryostat (both labeled 50 mK). Above the liquid

are “image” (1600 wafers) and “mask” (800 wafers) planes; these planes and their SQUID readouts constitute the coded aperture. The copper cryostat is lined with ~ 30 cm of solid nitrogen. A thin plastic sheet (labeled nylon here) serves only in the initial nitrogen freezing process. The outer cryostat, separated by vacuum and thermal shields, contains liquid nitrogen for cooling and as part of the outer gamma and neutron shield. Several meters of water completes the external shield in the laboratory. The relative thicknesses of the water and nitrogen will depend upon the details of the underground laboratory site. The total helium mass is 20 tonnes and the annual p-p and ${}^7\text{Be}$ event rate for a choice of a 5 tonne fiducial volume would be ~ 4500 events.

3 Background Sources and Strategies.

As was noted above the superfluid itself is a background-free target. Compton scattered gamma rays from any source external to the helium are the most dangerous background in liquid helium. The most important sources are: residual cosmogenic activity in the copper cryostat, primordial isotopes (U,Th,K) to varying degree in all the construction and shielding materials, gamma and neutron fluxes from the environment and products of penetrating muon-induced activity or capture in the container and shields. Products of muon interactions or capture in the liquid helium itself have negligible effect; at shallow depth dead times could be a difficulty for slow devices since wafers have a 10-20 msec relaxation. At the energies for most of the relevant gamma sources $> 90\%$ of the helium interactions are Compton scatters and of these the vast majority are multiple. Aside from careful shielding and material purity selection, several features of the gamma backgrounds can be exploited to minimize their effects in contaminating the signal or preventing an adequate background subtraction. These include: imposing a maximum total energy deposition cut ≤ 800 keV, rejection of events with multiple energy deposits and using the difference in spatial distribution of conversion points for neutrino signal and gamma background events arising from their very different mean free paths. Utilization of these effects requires good single event position determination and the ability to distinguish a major fraction of gamma events as multiple depositions. The strategy we have adopted attempts to achieve these capabilities by means of the coded aperture array and by the fact that a helium volume this large is nearly hermetic for gammas of these moderately low energies. Part of the purpose of the solid nitrogen lining the inner cryostat is to moderate (by Compton scatters in it) and shorten the mean free path for the remaining gamma flux from the copper cryostat which should now be dominant. Solid nitrogen has a density of 1.05 g-cm $^{-3}$ and has

no natural long-lived activity.

3.1 Backgrounds

Before discussing our progress toward these goals for dealing with backgrounds which have entered the helium, we discuss the external shields, muon effects and material purity requirements. For illustration it is useful to consider a particular site since the depth of overburden and laboratory wall content of primordial isotopes are the determining factors in overall configuration. At this writing the U.S. funding agencies have initiated a study to consider the creation of a national underground laboratory in the U.S. The Homestake Mine is one of the sites under active consideration so we use it at a depth of ~ 4500 mwe as an example. A muon flux of $4 \text{ m}^{-2}\text{-day}^{-1}$ is to be expected as are ambient gamma and neutron fluxes typical of hard rock facilities^{4,5}.

The materials in closest contact with the helium are the inner copper cryostat and its frozen nitrogen liner. We assume that the residual cosmogenic activity in the copper will be dominant and take as a design criteria for setting the allowed content of U/Th in it and in the nitrogen to be such that the contribution to the gamma flux is $\leq 10\%$ of that from the cosmogenics. The cosmogenic activity in the copper (e.g., ⁵⁴Mn, ⁵⁷Co and ⁶⁰Co) may be expected⁶ to be $\sim 50 \mu\text{Bq}$ under a manufacturing regime in which the material is above ground for 2 months and underground for 2 years. This rate implies a purity of $\leq 10^{-13} \text{ gm-gm}^{-1}$ for U/Th in the copper and $\leq 10^{-15} \text{ gm-gm}^{-1}$ for the solid nitrogen. Electroformed copper may satisfy this condition⁷. The recently developed¹⁰ cryo-adsorption filtering method for nitrogen while still liquid appears capable of achieving this level. The cosmogenic content of nitrogen is from ⁷Be (53 day half-life) which may be partly removed by the filtering but, since the nitrogen once frozen is not refreshed, the contribution to background is negligible after one year. The cosmogenics (e.g., ²²Na, ³H, ³²Si)^{8,9} in the wafer planes above the liquid, which will be either sapphire or silicon, are negligible contributors to background in the helium and their possible contribution to the event trigger rate by beta-decays in individual wafers is strongly suppressed by the multi-wafer coincidence requirement. Silicon can be obtained with very low ³²Si content⁹. As will be discussed below, these gamma background sources have been simulated and propagated into the helium using GEANT (ver.3.1416) for the cryostat geometry previously described.

Being a hard rock site an external water shield of 4 m thickness followed by 1 m of liquid nitrogen in the outer cryostat should be adequate for attenuation of external wall gamma and neutron flux^{11,12,13}. Although radon will not

diffuse into the cryogenic sections, its build up in the water should be avoided so water would be filtered and re-circulated at a modest rate. Optimization of all background effects for a specific site will no doubt use different relative amounts of water, liquid and solid nitrogen.

The muon induced activities in volumes of water and nitrogen of these sizes can be quite reasonably estimated for this site by calculation from known fluxes and cross sections¹⁵ and reference to recent accelerator experiments¹⁴ with high energy muon beams. The top of the water shield would be instrumented with phototubes for a muon veto of any activities with lifetimes ≤ 1 second in either the water, nitrogen, cryostat or helium. Of the potentially troublesome longer-lived activity in the outer water shield, ^{16}N , ^{15}O , ^{11}C , ^{14}O , there would be 139, 46, 13, 8 events per day, respectively in the water itself. The latter three are positron emitters. Within the solid nitrogen, there would be 1 event per day from the positron emitter ^{13}N with an additional 4 in the outer liquid nitrogen; other activities in both are negligible. A full Monte Carlo has not yet been done on the propagation of the decay products of these isotopes through the full detector and into the helium. However, we expect them to be a minor addition from our experience so far with calculations done for the inner cryostat and solid nitrogen moderator. Those GEANT simulations assumed, in addition to an ≤ 800 keV energy cut, that the coded aperture method would be able to distinguish multiple Compton scatters from neutrino-event-like single energy depositions if two scatters were separated by at least 15 cm in the helium, that effective event positions could be determined to that order and that a fiducial-non-fiducial statistical subtraction could be made. The gamma sources were taken to be those of the cosmogenics and primordials expected in the cryostat as described above. A typical signal and background recoil spectrum estimated for a 5 tonne fiducial volume, before subtraction, over a six month period is shown in Fig. 2.

3.2 Strategies

The principles of the coded aperture method were first described by Dicke³ and are now in wide use in imaging applications where the radiation cannot be focused or is of low intensity. In simple terms, the principle of operation is based on the concept of decoding an image formed on image plane pixels by the “shadow” of a mask plane constituting a pin-hole-like camera where the mask pattern and plane separation are known. A large modern literature exists and a large variety of mask patterns are employed². In our application there are important differences and simplifications in implementation. There are, of course, image and mask planes but here the “pixels” are wafer calorime-

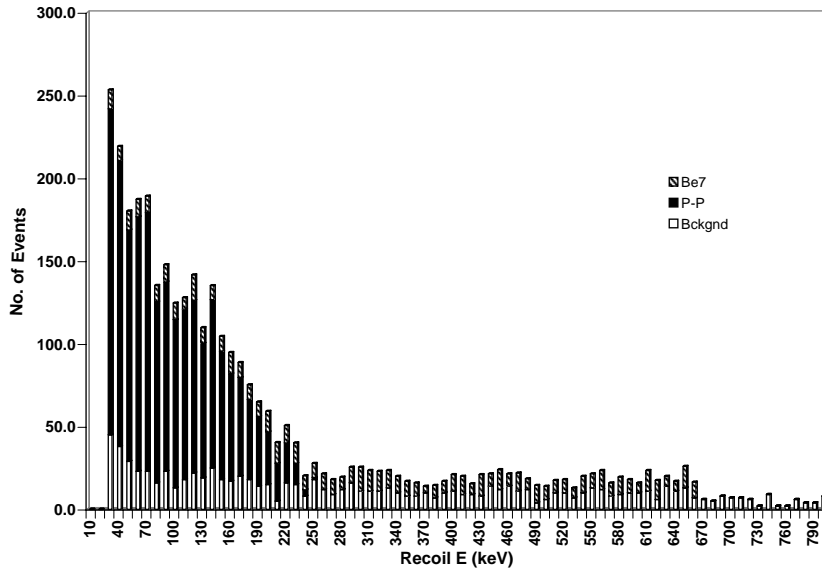


Figure 2. Expected recoil electron spectrum for a 5 tonne fiducial volume (6 mo.).

ters; the lower plane has 50% or more transmission. Unlike the usual method of coded apertures, the wafers forming the mask in HERON will also be active calorimeters and would be used in both position finding and energy determination. Thus no signal is lost by the presence of the mask. Depending on photon statistics a point source position can be found with varying precision. Two other tasks are required of the array: providing a fast event trigger and the ability to distinguish when the event is a distributed source rather than a point one. We are currently very actively pursuing two avenues to evaluate the likely effectiveness of the coded aperture method for background control. The first is directed toward achieving single, UV photon sensitivity on individual 12 cm wafers and the second is devoted to simulating a full scale coded aperture array of such wafers for developing and testing the most effective geometry and search algorithms for signal and background discrimination.

Space does not permit a full discussion of the wafer sensitivity work; however, it is based on the use of a tiny, magnetic metallic sensor attached to each of the wafers and is read-out by a SQUID. These devices have been developed at Brown in collaboration with scientists from University of Heidelberg and the Center for Astrophysics (Harvard-Smithsonian)¹⁶. The present status of

Table 2. Mean radial deviation from true position. (with energy at number of photons & depth given))

No. Photons→	500	200	75
Near top: (0.75 m)	3 cm (100 keV)	3 cm (44 keV)	5 cm (16 keV)
Near bottom: (4.5 m)	8 cm (533 keV)	13 cm (213 keV)	20 cm (77 keV)

the sensor performance is that a FWHM of 11 eV at 6 keV has been obtained on a device with smaller heat capacity and in a different geometry than we need but the results agree very well with calculation. These results suggest that the necessary single photon sensitivity may be achievable with these devices and new experiments are underway to adapt the success so far to sizes and geometries closer to our needs.

A point source at a given position would, with unlimited number of photons, give a unique pattern of intensities on the combination of mask and image planes. In order to achieve a recoil threshold energy of ~ 50 keV for events at the greatest depth in HERON only about 75 photons will hit the planes. Most events in the body of the detector will have 500 - 10,000 photons. As a consequence we have taken a maximum likelihood approach to finding the the best position of a single event and also to make a measure of the probability that it is not from a point source and is therefore background. The simulation uses a HERON geometry as described above. For an event of a given number of photons and assumed initial position the fractional solid angles for each pixel ($\Delta\Omega_{ij}/\Omega$) in both planes are known as are the number of photons (n_{ij}). Consequently, we write a likelihood function $L(xyz)$ of the form:

$$L(xyz) = \prod \frac{(\Delta\Omega_{ij}/\Omega)^{n_{ij}}}{n_{ij}!} \quad (2)$$

To test the position finding accuracy we generate point source events covering the full range of expected photon intensity and from all regions of the helium volume. The search algorithm converges rapidly and, except at the extremities, find positions to within a few cm. The results so far for the precision with which the event position can be found are very promising and a few examples are given in Table 2. We are now in the process of testing variations of this likelihood technique for its ability to distinguish background events from signal events when the former have multiple depositions of energy. To do this we must generate a realistic sample of background conversions in the helium. GEANT (ver. 3.1416), with the same HERON geometry and gamma

spectrum as in the discussion above of cosmogenic background from the cryostat, is used for this purpose. It is also essential to test these discrimination algorithms in a way that closely resembles the level of information that will be available in a real experiment. For example, because of the statistical nature of the hit patterns, the event pattern actually recorded is only one of a large ensemble of hit patterns possible for any particular energy deposition in the detector. This is the pattern (including pulse heights) available for analysis. Acting on this information an effective-single-event position is found and the value of its likelihood known. Thus there are a range of likelihood values for a given background event and also for a point source of the same energy and effective-single-event position. Among the questions to be answered is: what are the ranges of the likelihood values for any particular background event and for those of its effective-single-event with the same number of photons and to what extent are the two event types distinguishable on likelihood criteria. We have preliminary results on this question based on a modest size sample of GEANT-generated events. Fig. 3 shows the log-likelihood distribution for a 5361 photon background event. In the event in Fig. 3, 80% of the total event

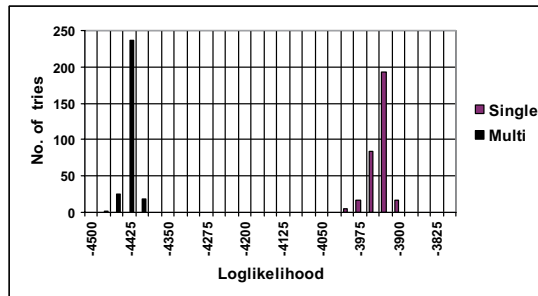


Figure 3. Log-likelihood distribution for 5361 photon background event.

energy of was contained in only 2 Compton conversions with the remaining energy distributed among another 6 Comptons. The major depositions were only 29 cm apart. The entire event is at a mean depth of 3.2 m. The left hand distribution results from generating a sequence of patterns for the original event and the right hand one corresponds to that for the effective-single solutions found as would be in a real experiment. The separation is clear having a mean log-likelihood separation of 573. As the photon multiplicity decreases the separation deteriorates somewhat and is dramatically better for higher photon multiplicities. The sample of representative background events

must be increased before a conclusion can be reached on the quantitative level of signal to noise discrimination achievable by this method at the lowest photon multiplicities of a full size detector. However, on the evidence so far the method is showing promise. There is additional information which can be incorporated into this type of approach. Although we use the delayed roton/phonon signal in the energy determination, so far we have included only the photon information in the discrimination algorithm. Whether it is preferable to include the roton/phonon data into this type of approach or rather into a separate, complementary one is still to be considered.

4 Summary

The principles of operation and the physical configuration of a HERON detector currently in R&D for measuring the total flux and recoil energy spectrum of p-p and ^7Be are described. Particular emphasis is given to current progress on methods to control backgrounds. Our present efforts are concentrating on achieving single photon sensitivity and on testing the coded aperture event finding technique. We are eager to have additional collaborators join in the many interesting physics aspects of the project and in its application to the new, p-p solar neutrino frontier.

Acknowledgments

This work was supported in part by the U.S. Department of Energy under grant DE-FG02-88ER40452. We wish also to thank the conference organizers for their invitation to participate and their hospitality during the workshop.

References

1. S. Bandler *et al*, *Phys. Rev. Lett.* **74**, 3169 (1995); C. Enss *et al*, *Physica B* **194**, 515 (1994); J. Adams *et al*, *Phys. Lett.* **B341**, 431 (1995); J. Adams *et al*, *Nucl. Instrum. Methods* **B444**, 51 (2000).
2. E. Fenimore and T. Cannon, *Appl. Optics* **17**, 337 (1974).
3. R. Dicke, *Astroph. J.* **153**, L101 (1968).
4. C. Arpesella *et al*, *Nucl. Phys.* **A 28**, 420 (1992).
5. P. Belli *et al*, *Nuovo Cim.* **101A**, 959 (1989).
6. G. Heuser in *3rd Intl. Workshop on Low Radioactivity in the Environment*, ed. M. Garcia-Leon & R. Garcia-Tenorio, (World Scientific, Singapore, 1994).

7. Using isotope dilution mass spectrometry we have measured $\leq 10^{-12}$ gm-gm⁻¹ in a sample of electroformed copper.
8. C.J. Martoff, *Science* **237**, 507 (1987).
9. R. Plaga *et al*, *Nucl. Instrum. Methods A* **309**, 598 (1991).
10. G. Heuser *et al*, *Appl. Rad. & Isotopes* **52**, 691 (2000).
11. J. Boger *et al*, *Nucl. Instrum. Methods A* **449**, 172 (2000); Sudbury Neutrino Observatory proposal SNO-87-12.
12. G. Alimonti *et al*, *Astropart. Phys.*, submitted 27 Nov. 2000; C. Arpesella *et al*, Proposal for a Real-time Detector for Solar Neutrinos (Borexino) (INFN, Milano 1991).
13. L. Baudis *et al*, *Nucl. Instrum. Methods A* **426**, 425 (1999).
14. T. Hagner *et al*, *Astropart. Phys.* **14**, 33 (2000).
15. See for example, for muon and neutron fluxes and energies underground: M. Ambrosio *et al*, *Astropart. Phys.* **10**, 11 (2000); F. Boehm *et al*, *Phys. Rev. D* **62**, 1103 (2000); M. Aglietta *et al*, hep-ex/990547; and M. Aglietta *et al*, *Nuovo Cim. C* **12**, 467 (1989); T.K. Gaisser, *Cosmic Rays and Particle Physics*, Cambridge University Press (1990); V. McLane *et al.* in *Neutron Cross Sections* (Academic Press, Boston 1988); Y-F. Wang *et al*, hep-ex/0101049 and ref. therein. For muon capture and cross sections: R. Cohen *et al*, *Nucl. Phys.* **57**, 255 (1964); L. Bergamasco *et al*, *Nuovo Cim. A* **67**, 255 (1982); S. Charalambus, *Nucl. Phys. A* **166**, 145 (1970); T. Suzuki *et al*, *Phys. Rev. C* **35**, 2212 (1987); V. di Napoli *et al*, *Phys. Rev. C* **8**, 206 (1973); J. O'Connell & F. Schima, *Phys. Rev. D* **38**, 2277 (1988).
16. S. Bandler *et al*, *J. of Low Temp. Phys.* **93**, 709 (1993); A. Fleischmann *et al*, *Nucl. Instrum. Methods B* **444**, 100 (2000).